International Journal of Medical, Medicine and Health Sciences
ISSN: 2517-9969
Vol:8, No:9, 2014

Effects of Data Correlation in a Sparse-View Compressive Sensing Based Image Reconstruction

Sajid Abbas, Joon Pyo Hong, Jung-Ryun Lee, Seungryong Cho

***Abstract*—**Computed tomography and laminography are heavily investigated in a compressive sensing based image reconstruction framework to reduce the dose to the patients as well as to the radiosensitive devices such as multilayer microelectronic circuit boards. Nowadays researchers are actively working on optimizing the compressive sensing based iterative image reconstruction algorithm to obtain better quality images. However, the effects of the sampled data's properties on reconstructed the image's quality, particularly in an insufficient sampled data conditions have not been explored in computed laminography. In this paper, we investigated the effects of two data properties i.e. sampling density and data incoherence on the reconstructed image obtained by conventional computed laminography and a recently proposed method called spherical sinusoidal scanning scheme. We have found that in a compressive sensing based image reconstruction framework, the image quality mainly depends upon the data incoherence when the data is uniformly sampled.

***Keywords*—**Computed tomography, Computed laminography, Compressive sending, Low-dose.

I. Introduction

IN computed tomography (CT) the choice of image reconstruction algorithms are either analytic or iterative. The former image reconstruction technique estimates the missing data from the sampled data set and the latter computes the imaging model iteratively from the sampled data set to obtain the objective function. Additionally, a compressive sensing (CS) based iterative image reconstruction algorithm exploits the sparsity of objective function and enables successful image reconstruction from an incomplete data set, whereas an analytic algorithm - such as the Feldkamp, Davis, and Kress (FDK) algorithm - in such insufficient data conditions results in streak artifact in the reconstructed images.

The CS-based image reconstruction algorithm has shown promise using sparsely sampled data and provides a solution to reduce the scanning time and radiation dose to both the patient and radiosensitive devices (such as flash ram, multi-layer printed circuit board) in CT and computed laminography (CL), respectively [1]-[4]. These days, researchers are actively working on optimizing the CS-based image reconstruction algorithm to improve the reconstructed image quality, convergence speed and to eliminate the reconstruction parameters by implementing convex optimization approaches [5]-[7]. In addition to that, optimization of scanning schemes have not been much investigated in CT or CL in a CS- based image reconstruction framework. In CT, Abbas et al. [8] emphasized the importance of data property of the sparsely sampled data in a CS-based image reconstruction framework.

In this work, we demonstrate the importance of data correlation in CL. For this purpose we implemented two CL scanning schemes i.e. conventional CL scanning scheme or oblique CT and a newly presented spherical sinusoidal sampling scheme as shown in Figs. 1 (a) and (b), respectively. Spherical sinusoidal scanning scheme is an upgraded version of oblique CT, and its outperformance in the sparse sampling case has been demonstrated [2]. In this simulation study, we implemented a CS-based total-variation (TV) minimization algorithm [3]-[9] for the image reconstruction of both the sampling schemes and analyzed the reconstructed images both qualitatively and quantitatively emphasizing the effects of data correlation.

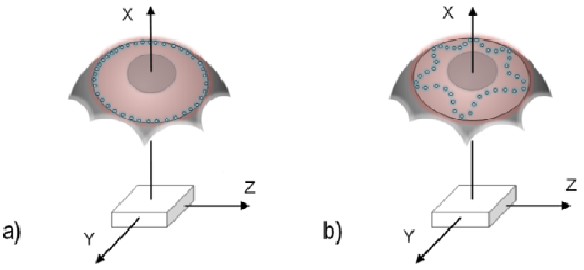

Fig. 1 Geometric illustration of oblique and spherical sinusoidal scanning configurations in 3D Cartesian coordinate

II. Methods

A. Scanning Schemes

CL is actively used in the nondestructive testing of flat objects. CL is a generalization of CT such that the source is tilted to an angle θ away from the source rotation axis, for example, around X-axis in Fig. 1. In this work we set the source tilt angle to 30 degrees. In comparison to conventional CL approach, in spherical sinusoidal scanning scheme, source to rotation axis distance is continuously varying during a scan in a sinusoidal fashion with respect to source rotation angle as

S. Abbas, J. P. Hong, and S. Cho are with the Department of Nuclear and Quantum Engineering, Korea Advanced Institute of Science and Technology, Daejeon, South Korea (e-mail: scho@kaist.ac.kr).

J. -R. Lee is with the School of EEE, Chung-Ang University, Seoul, South Korea.

The authors are grateful to the support in part by the National Research Foundation of Korea funded by the Ministry of Science, ICT & Future Planning NRF-2013M2A2A9043476 and NRF-2011-0030450. Lee was supported by the MSIP (Ministry of Science, ICT & Future Planning), Korea, under the ITRC (Information Technology Research Center) support program (NIPA-2014-H0301-14-1015) supervised by the NIPA (National ICT Industry Promotion Agency).

shown in Fig. 1 (b). In spherical sinusoidal scanning scheme we set the source tilt angle to vary between 5 and 30 degrees.

B. Test Resolution Phantom

We developed a resolution test phantom similar to the one used in Xu's work [10]. The dimensions of the phantom are 2.0cm x 4.0cm x4.0cm. We placed 14 high contrast boxes in the center of a large rectangular box and stacked them in an increasing aspect ratio towards the source. The maximum and minimum heights of the boxes were set to 1.56mm and 0.46mm. The attenuation values of background and high contrast boxes were set to 1.0 and 3.0. The size of the reconstructed image volume is 128x256x256. Each side of the detector was 32.0cm long and discretized to a 2D array of 512 x 512 pixels.

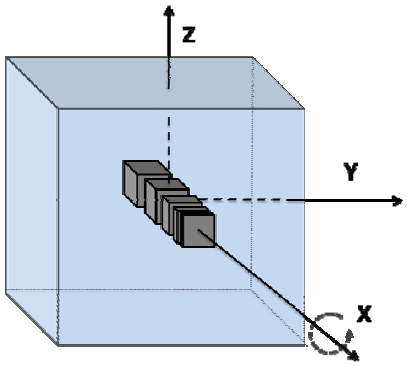

Fig. 2 Schematic diagram of numerical resolution-test phantom

The source to rotation axis and source to detector distances were set to 25cm and 55cm. The projection data was collected on regular interval using full-view and sparse-view scanning protocols at 360 and 40 views, respectively.

C. Reconstruction Algorithm

In this simulation study, we implemented the TV minimization algorithm which was originally implemented by Sidky et al. [3], [9] for a circular cone-beam scanning scheme. The objective function of the TV minimization algorithm is to minimize the l_1 −norm of magnitude of image derivative. The solution of the optimization problem $\hat{\vec{x}}$ can be defined as below:

$$\hat{\vec{x}} = argmin\|\vec{x}\|_{TV}\ s.t.\ \|A\vec{x} - \vec{g}\| < \varepsilon \qquad (1)$$

where $\vec{x}$ is the image under reconstruction and A is the system matrix contains the weights to describe the ray integrals. $\vec{g}$ represents the actual measurement. TV minimization algorithm consists of two steps. The first step is projection-onto convex-sets (POCS) which performs two tasks. The first one is to take care of data consistency constraint i.e. the difference between actual and calculated projection in back projection module should be less than the defined error ε. The second task is to find the image pixels with negative values in the reconstruction volume and replacing those negative values with zero before going to the second main step of the TV minimization algorithm i.e. TV step. In the TV step, the gradient of the image TV is calculated for gradient descent method to find the new search direction in an attempt to find the minimum image solution. Therefore in TV step the objective function of TV minimization algorithm is satisfied by minimizing the l_1 −norm of magnitude of image derivative.

III. Results

The reconstructed images of the resolution test phantom using the full-view scanning protocol data for oblique and spherical sinusoidal scanning schemes are shown in Fig. 3.

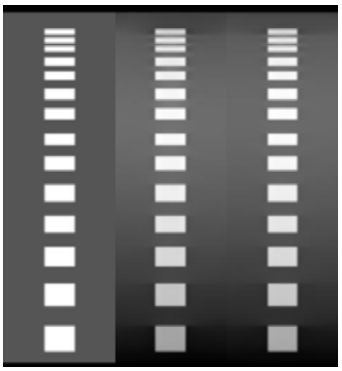

Fig. 3 Reconstructed images of resolution-test phantom from data at 360 views. Images are arranged in an order starting from left to right with ground truth, reconstructed images by oblique and spherical sinusoidal schemes

It appears that both the reconstructed images are similar to each other and are in good comparison with the reference image. Similarly using the sparse-view scanning protocol data, the reconstructed images of the resolution test phantom for oblique and spherical sinusoidal scanning schemes are shown in Fig. 4.

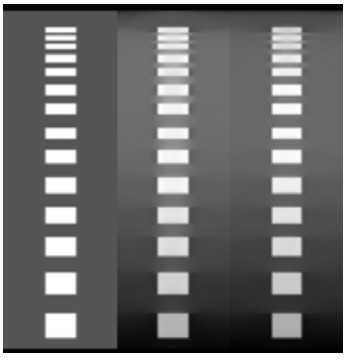

Fig. 4 Reconstructed images of resolution-test phantom from data at 40 views. Images are arranged in an order starting from left to right with ground truth, reconstructed images by oblique and spherical sinusoidal schemes

One can notice that the reconstructed image of resolution-test phantom obtained by spherical sinusoidal scanning scheme shows a better image contrast than compared to

oblique scanning scheme.

In addition to that we also performed a quantitative analysis by calculating SIMM values [11]. The SSIM measures the degree of similarity in structure, luminance and contrast among the reference and target images. Its value varies between 0 and 1. If the SSIM value is 1, the two images are similar to each other, whereas if its value is 0 i.e. the two images have nothing in common.

TABLE I
SSIM INDEX VALUES OF THE RECONSTRUCTED IMAGES

No of views	Scanning Schemes		Difference
	Oblique CT	Spherical Sinusoidal	
360	0.978	0.978	0.0
40	0.842	0.900	0.058

The SSIM values for both the scanning schemes are presented in Table I. The SSIM values in case of sampled data at 360 views are the same for both the scanning schemes. The SSIM values of Fig. 4 confirm that the spherical sinusoidal scheme outperforms the conventional scanning scheme in an insufficient data condition i.e. in case of sampled data at 40 views used for image reconstruction.

IV. DISCUSSION

The focus of this paper is to demonstrate and highlight the importance of the effects of sampled data properties in the CS-based CL image reconstruction. We analyzed both the CL scanning schemes i.e. oblique and spherical sinusoidal sampling schemes by two metrics i.e. sampling density and data incoherence [9]. The oblique and spherical sinusoidal scanning schemes both uniformly sampled the target of interest.

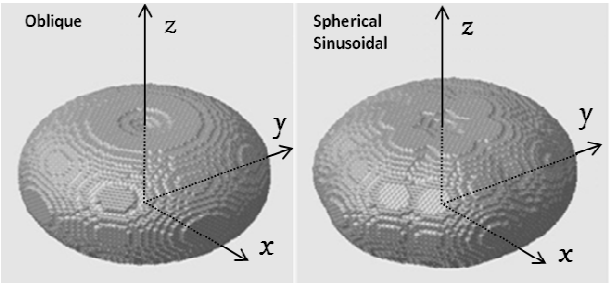

Fig. 5 3D radon space for oblique and spherical sinusoidal scanning scheme

This can be confirmed by looking into Fig. 5 which shows almost same reciprocal space coverage is provided by both the sampling scheme. In other words both the sampling schemes provide the same sampling density. In such scanning condition, if sufficient data is available, successful image reconstruction is always guaranteed. The reconstructed images of the resolution-test phantom in Fig. 3 confirm this fact. But what would happen if the uniformly sampled data acquired by both the sampling schemes is sparse? A drop in image contrast can be noticed in the reconstructed images shown in Fig. 4 because the sampling density was reduced to 1/9 of the fully sampled data set.

Interestingly, it can be noticed in Table I that SSIM values of both the sampling schemes are same in the case of sampled data used at 360 views for image reconstruction. However a larger drop of 0.058 in SSIM value of oblique scheme compared to spherical sinusoidal scanning scheme can be observed in case of sampled data used at 40 views for image reconstruction. The reason why spherical sinusoidal scheme outperforms the oblique scanning scheme in case of sampled data at 40 views is due to the fact that the sampled data obtained by spherical sinusoidal is more incoherent compared to that obtained by oblique scanning scheme.

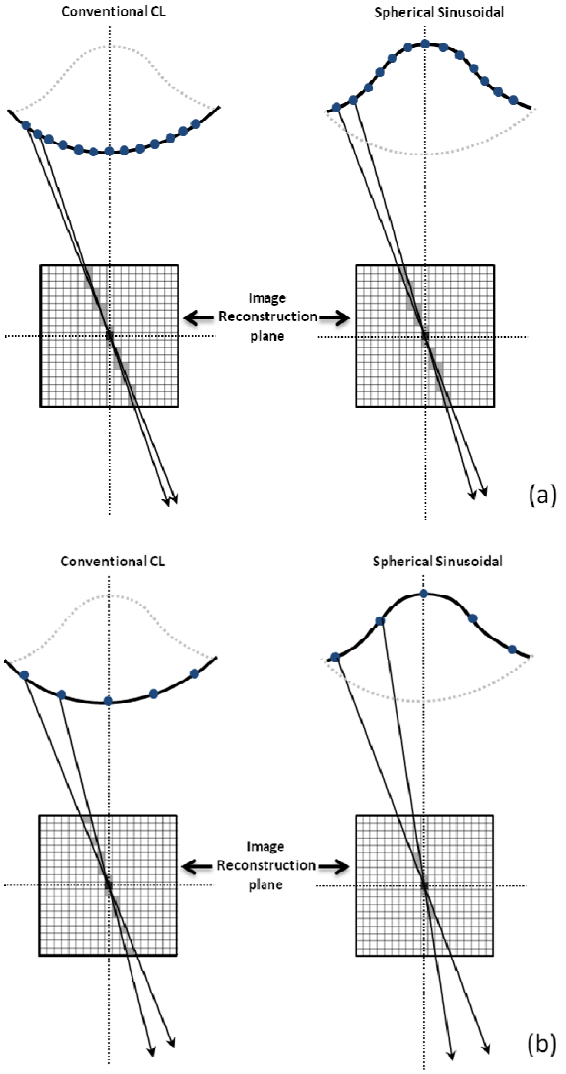

Fig. 6 Schematic illustration of data correlation in sampled data

In Fig. 6 one can see a portion of source trajectory circumference of both the scanning schemes. In case of spherical sinusoidal the portion of circumference compared to oblique scanning scheme is larger. It means that sampling points were located close to each other in case of oblique compared to spherical sinusoidal scanning scheme. For better

visualization and understanding, only one ray was drawn from two of the neighboring sampling points that pass through the image pixel present in the center (marked by a black color) of a 2D image plane as shown in Fig. 6. We highlighted the image pixels in gray that were sampled by both the rays. In the case of sampled data at 360 views, sampling points were located so close each other that the difference between the two sampling points in both sampling schemes is almost the same like shown in Fig. 6 (a). In this state, it is more likely that we get almost the same data correlation within the sampled data set obtained by both sampling schemes. Whereas, as one can see in Fig. 6 (b) the sampling points are located more far apart in case of spherical sinusoidal than compared to oblique scanning scheme. Therefore, there is a greater chance that we may find more correlated (more gray pixels) sampled data in case of oblique compared to spherical sinusoidal scheme. The data correlation is important because it may not provide additional information in a CS-based image reconstruction. In summary, the performance of CS-based image reconstruction algorithm is proportional to the given number of rays per pixel provided that the rays are highly incoherent.

V. Conclusion

In this work we qualitatively and quantitatively compared the two CL scanning schemes i.e. oblique and spherical sinusoidal schemes. We have found that the spherical sinusoidal outperforms the oblique scanning scheme in cases of insufficient data condition, for example in case of data set at 40 views in present study. We conjectured that the larger drop in image contrast of the reconstructed images of the resolution-test phantom obtained by oblique scanning scheme compared to spherical sinusoidal scanning scheme is due to the presence of more correlation among the sampled data set. Therefore, care must be taken while devising the CT or CL scanning schemes so that the sampled data obtained by them should be as much incoherence as possible. In addition to that, spherical sinusoidal scanning scheme may provide solution of fast and low-dose non-destructive testing to radio-sensitive devises.

Acknowledgment

The authors would like to thank Park Miran and Taewon Lee for their helpful discussion.

References

[1] S. Abbas, J. Min, and S. Cho, “Super-sparsely view-sampled cone-beam CT by incorporating prior data,” *J. X-Ray Sci. Technol.*, vol. 21, pp. 71–83 (2013).

[2] S. Abbas, M. Park, J. Min, H. K. Kim, and S. Cho, "Sparse-view computed laminography with a spherical sinusoidal scan for nondestructive testing," *Opt. Express* (Accepted: 24 June,2014).

[3] E.Y. Sidky, C.-M. Kao, and X. Pan, “Accurate image reconstruction from few-views and limited-angle data in divergent-beam CT,” *J. X-Ray Sci. Tech.*, vol. 14, pp. 119-139 (2006).

[4] S. Cho, T. Lee, J. Min, and H. Chung, “Feasibility study on many-view under sampling (MVUS) technique for low-dose computed tomography,” *Opt. Eng*., vol. 51, pp. 080501 (2012).

[5] E. Y. Sidky, J. H. Jørgensen, and X. Pan, “Convex optimization problem prototyping for image reconstruction in computed tomography with the Chambolle-Pock algorithm,” *Phys. Med. Biol.*, vol. 57, pp. 3065-3091, 2012.

[6] J. C. Park, B. Song, J. S. Kim, H. K. Kim, Z. Liu, T. S. Suh, and W. Y. Song, "Fast compressed sensing-based CBCT reconstruction using Barzilai-Borwein formulation for application to on-line IGRT," *Med. Phys.*, vol. 30, pp. 1207- 121, 2012.

[7] T. Niu and L. Zhu, "Accelerated barrier optimization compressed sensing (ABOCS) reconstruction for cone-beam CT: Phantom studies," *Med. Phys.*, vol. 39, pp. 4588-4598, 2012.

[8] S. Abbas, T. Lee, S. Shin, R. Lee, and S. Cho, “Effects of sparse sampling schemes on image quality in low-dose CT,” *Med. Phys.* vol. 40, pp. 111915 (2013).

[9] E.Y. Sidky and X. Pan, “Image reconstruction in circular cone-beam computed tomography by constrained, total-variation minimization,” *Phys. Med. Biol*. vol. 53, pp. 4777-4807 (2008).

[10] F. Xu, L. Helfen, T. Baumbach, and H. Suhonen, “Comparison of image quality in computed laminography and tomography,” *Opt. Express* vol. 20 , pp. 794-806 (2012).

[11] Z. Wang, A. C. Bovik, H. R. Sheikh, and E. P. Simoncelli, “Image quality assessment: From error visibility to structural similarity,” *IEEE Trans. Image Process.* vol. 13, pp. 600-612 (2004).